The RNA-binding protein Vg1 RBP is required for cell migration during early neural development

Karina Yaniv[1], Abraham Fainsod[2], Chaya Kalcheim[1] and Joel K. Yisraeli[1,*]

[1]Department of Anatomy and Cell Biology, Hebrew University – Hadassah Medical School, POB 12272, 91120 Jerusalem, Israel
[2]Department of Cellular Biochemistry and Human Genetics, Hebrew University – Hadassah Medical School, POB 12272, 91120 Jerusalem, Israel
*Author for correspondence (e-mail: yisraeli@cc.huji.ac.il)

Accepted 6 August 2003

Development 130, 5649-5661

doi:10.1242/dev.00810

Summary

After mid-blastula transition, populations of cells within the *Xenopus* embryo become motile. Using antisense morpholino oligonucleotides, we find that Vg1 RBP, an RNA-binding protein implicated in RNA localization in oocytes, is required for the migration of cells forming the roof plate of the neural tube and, subsequently, for neural crest migration. These cells are properly determined but remain at their site of origin. Consistent with a possible role in cell movement, Vg1 RBP asymmetrically localizes to extended processes in migrating neural crest cells. Given that Vg1 RBP is a member of the conserved VICKZ family of proteins, expressed in embryonic and neoplastic cells, these data shed light on the likely role of these RNA-binding proteins in regulating cell movements during both development and metastasis.

Key words: VICKZ protein family, RNA-binding proteins, Neural crest, Roof plate, Cell movement, *Xenopus*

Introduction

Asymmetric distribution of RNA within cells has been observed in a wide variety of embryonic and somatic cells. Such localized RNAs provide an efficient means for creating a heterogeneous distribution of protein through the translation of specific RNAs at particular, intracellular locations. RNAs are sorted within cells via interactions with specific RNA-binding proteins and cytoskeletal elements. Vg1 RBP (also known as Vera) is one such RNA-binding protein that has been implicated in the intracellular localization of *Vg1* RNA to the vegetal cortex of *Xenopus* oocytes (Havin et al., 1998; Deshler et al., 1998). Vg1 RBP recognizes cis-acting elements in the 3′ UTR of *Vg1* RNA (Bubunenko et al., 2002; Deshler et al., 1998; Deshler et al., 1997; Havin et al., 1998; Kwon et al., 2002; Mowry, 1996; Schwartz et al., 1992) and is likely to facilitate localization by mediating its association with microtubules in oocytes (Elisha et al., 1995). *Vg1 RBP* mRNA is also expressed in a number of cell types during embryogenesis, although the role of the protein in these different tissues has not been examined (Mueller-Pillasch et al., 1999; Zhang et al., 1999).

Over the past few years, it has become clear that Vg1 RBP is a member of a family of RNA-binding proteins, which we have termed VICKZ proteins, based on the first letters of the founding members of this family (Vg1 RBP/Vera; IMP-1, IMP-2 and Imp-3; CRD-BP; KOC; and ZBP-1) (Yaniv and Yisraeli, 2002). These proteins are highly conserved among all vertebrates that have been examined, in both their primary sequence and their expression patterns during embryogenesis (Mueller-Pillasch et al., 1999; Zhang et al., 1999). All family members contain two RNA recognition motifs (RRMs) at their N terminus, an RGG RNA-binding domain and four hnRNP K-homology (KH) domains at the C terminus (also shown to mediate RNA binding in other proteins). In chick embryo fibroblasts, a homolog, termed ZBP-1, binds *β-actin* mRNA and co-localizes with this RNA to the leading edge of migrating cells (Farina et al., 2003; Oleynikov and Singer, 2003; Ross et al., 1997). Other members of the VICKZ family are involved in RNA stability (CRD-BP) (Leeds et al., 1997) and translational control (IMP-1, IMP-2 and IMP-3) (Nielsen et al., 1999) in different embryonic cell types. Quite strikingly, a number of different types of human cancers and neoplastic cells overexpress one or more of the three human homologs of the VICKZ family, yet their role in cancer cells is not understood (reviewed by Yaniv and Yisraeli, 2002). The expression in almost all normal adult tissues is essentially non-detectable, however; based on this expression profile, the VICKZ proteins have been termed ‘oncofetal proteins’.

The biological function of VICKZ proteins is beginning to be deciphered. In embryonic hippocampal neurons, ZBP-1 protein and *β-actin* mRNA colocalize in growth cones (Zhang et al., 2001a). In these cells, an antisense oligonucleotide directed against *β-actin* RNA localization (‘zipcode’) sequences found in its 3′UTR disrupts both *β-actin* RNA and ZBP-1 protein localization and leads to growth cone collapse. The same antisense oligonucleotide, in migrating embryo fibroblasts in culture, causes a loss of lamellar ZBP-1 localization, cellular polarity and persistent movement (Kislauskis et al., 1994; Kislauskis et al., 1997; Oleynikov and Singer, 2003; Shestakova et al., 2001). These experiments, although indirect, suggest that VICKZ proteins play a role in cell migration via their ability to localize RNA. Cell movement requires the coordinated regulation of a number of different processes within the cell. At the leading edge, increased actin

polymerization leads to an extension of the cell membrane and the formation of new focal contacts with the substratum (reviewed by Welch et al., 1997). At the trailing edge, focal contacts are broken, the cell membrane is retracted, and the cell mass moves forward. During cell migration, a number of proteins, many of which are involved in signal transduction or actin nucleation or polymerization, are localized and/or activated at either the leading or trailing edge. By sorting requisite RNAs to particular intracellular targets, cells could facilitate the local production of proteins needed for prolonged, persistent migration.

In *Xenopus* embryos, cell motility is activated at the mid-blastula transition (Gerhart, 1979). The embryo undergoes a series of cell shape changes and migrations that transform it from a sphere into a tadpole with a clearly defined anteroposterior bilateral axis of symmetry. Cells arising in the lateral edges of the neural plate demonstrate a great deal of motility, with cells from the superficial layer migrating medially to form the dorsal domain of the neural tube, and those from the deep layer migrating along defined pathways throughout the embryo as neural crest cells (Davidson and Keller, 1999). As shown for many cell movements, neural crest cell migration is dependent on an intact actin cytoskeleton and signalling apparatus (Liu and Jessell, 1998; Santiago and Erickson, 2002).

We decided to directly explore the role of Vg1 RBP in *Xenopus* embryos and explants. Neural crest migration is severely diminished in embryos in which the level of Vg1 RBP expression has been reduced by injecting antisense morpholino oligonucleotides (AMOs). Other specific defects are also observed, including a dorsally open neural tube that appears to derive from the inability of correctly specified neuroepithelial cells to reach the dorsal midline. In explants, Vg1 RBP is localized to the distal edge of emigrating neural crest, and this process is inhibited in neural tubes explanted from antisense-injected embryos. Our results, reducing for the first time the expression of a VICKZ family member in developing embryos show that these proteins play a role in cell migration in different cell types.

Materials and methods

Neural crest cell culture

Neural primordial containing pre-migratory neural crest cells were explanted and cultured essentially as described (Fukuzawa and Ide, 1988), with some modifications. *Xenopus* embryos of stage 20/22 were dejellied and decapsulated in sterile Steinberg's balanced salt solution (BSS) (Elsdale and Jones, 1963). Each embryo was divided horizontally into two pieces along the notochord, and a caudal portion of the dorsal piece, containing the neural tube, was transferred, for 30 minutes, to Steinberg's BSS containing 0.1% collagenase, in order to facilitate the subsequent removal of the surrounding tissues from the neural tube. The neural tube was then cut, followed by removal of the epidermis, somites, and notochord, and then cultured overnight at 25°C in a drop of about 50 μl of medium, on a fibronectin-coated tissue culture dish. The culture media contained Steimberg's BSS (89%), Leibowitz medium (10%) supplemented with 1 mM L-glutamine, 100 μg/ml gentamycin and fetal calf serum (1%).

Immunofluorescence

Cultured neural crest cells were fixed in MEMFA (0.1 M MOPS, pH 7.4, 2 mM EGTA, 1 mM $MgSO_4$ and 3.7% Formaldehyde) for 30 minutes and immunostained overnight at 4°C with rabbit anti-Vg1RBP antibody (Zhang et al., 1999) at a 1:100 dilution. For staining with monoclonal antibody HNK-1, the cells were fixed in 4% paraformaldehyde. The plates were incubated for 1 hour at room temperature with the secondary antibody (1:100), consisting of either affinity-purified goat anti-mouse or anti-rabbit IgG conjugated to cy5 or rhodamine, respectively (Jackson Immunoresearch). Slides incubated with the secondary antibody alone showed no background fluorescence. Coverslips were mounted in Glycerol:PBS (1:1).

In situ hybridization and probes

Embryos were fixed in MEMFA and processed for whole-mount in situ hybridization as described elsewhere (Epstein et al., 1997), or for hybridization to sections as described previously (Butler et al., 2001). Embryos destined for paraffin sectioning were stained with NBT/BCIP (20 μl/ml from stock solution; catalog number 1681451, Roche) instead of magenta phosphate. Staining reactions were never allowed to proceed beyond the point that embryos incubated in parallel with control probes were completely negative. Probes were prepared with the RiboMax Transcription Kit (Promega) using Digoxygenin-UTP (Roche) and subsequently cleaned using the RNA Easy Kit (Qiagen). The probes used were: *Xsnail*, the SP72Xsna plasmid (Sargent and Bennett, 1990); *Vg1 RBP*, a 609 bp probe spanning amino acids 282-485 of *Xenopus* Vg1 RBP; *pax3*, PCR fragment spanning amino acids 41-267 of mouse Pax3 (Goulding et al., 1991) and *Xtwist*, a 560 bp probe (Hopwood et al., 1989).

Manipulation and injection of embryos

Eggs were stripped, fertilized and injected as previously described (Epstein et al., 1997). Embryos were maintained in 0.1× Modified Barth's Solution-HEPES (MBSH) and, at the two-cell stage, they were transferred to 1× MBSH for injection. Morpholino oligonucleotides, either directed against a sequence in the 5′UTR of *Vg1 RBP* (5′AAAGAAGACGAGCCCGAAAAACCCG3′) or encoding a control sequence (5′CCTCTTACCTCAGTTACAATTTATA3′), were purchased from Gene Tools LLC, resuspended in sterile, filtered water and 10ng/blastomere was injected into either one or both blastomeres. For the rescue experiments, 1.4 ng of capped *Vg1 RBP-GFP* RNA, synthesized using the Cap Scribe RNA kit (Roche) from a pET21-Vg1 RBP plasmid (obtained from A. Git), was co-injected with AMO into each blastomere of a two-cell stage embryo. The *Vg1 RBP-GFP* mRNA lacks all 5′ and 3′ UTR sequences, and is therefore not a target for AMO-directed inhibition of translation. For the overexpression experiments, 2 ng/blastomere of *Vg1 RBP-GFP* RNA was injected. Both injected and uninjected embryos were staged according to Nieuwkoop and Faber (Nieuwkoop and Faber, 1967), and not on the basis of elapsed time from fertilization.

Microinjection of DiI

Stage 16 embryos were dejellied manually prior to injections, which were carried out in 0.1× MBSH. Cell Tracker CM-DiI [C-7001, Molecular Probes; 4 nl from a 1mg/ml stock solution (in 100% ethanol)] was injected into the dorsal neural folds, containing presumptive neural crest and roof plate cells (Collazo et al., 1993). Following the injection, the embryos were maintained at 17°C until stage 34, when they were fixed and photographed using a fluorescent stereoscope. A rhodamine filter set was used to detect the dye. For the single blastomere injections (Fig. 5D-F), 0.4 ng of capped *GFP* mRNA was co-injected with 10 ng of AMO into one blastomere at the two-cell stage and, at stage 16, labeled with DiI, as above. Embryos were fixed and photographed at stage 28.

Optical and histological sections

For confocal sections, embryos were labeled at the one-cell stage by injection of 4 nl from a stock solution (10 mg/ml of water) of Alexa Fluor 647-Dextran (anionic, fixable; Molecular Probes). Following the injection, the embryos were returned to 0.1× MBSH and maintained at 17°C until they reached the desired stage. Following

fixation in MEMFA, embryos were cut transversely into several pieces as described (Davidson and Keller, 1999). The pieces were dehydrated through a dehydration series into 100% methanol and placed in disposable chambers constructed by gluing nonmagnetic nylon washers (catalog number B-WNA-3/8N, Small Parts, http://www.smallparts.com) to form a well on a no. 0 coverslip (Marienfeld). The samples were then cleared and oriented as described (Davidson and Keller, 1999). Optical sectioning was performed immediately after mounting, using a confocal scanning laser system attached to an inverted compound microscope (40× objective).

For histological sections, fixed or stained embryos (after in situ hybridization) were embedded in paraffin wax and sectioned at 10 μm thickness.

Western blot analysis

Two embryo equivalents per lane of an S10 protein extract were resolved on a 10% SDS-PAGE gel, transferred to an Immobilon membrane and probed with 1:20,000 of a Vg1 RBP polyclonal serum, followed by a horseradish peroxidase-coupled goat anti-rabbit antibody and ECL detection. Blots were then stripped by standard protocols and probed with a 1:10,000 dilution of ERK-2 monoclonal antibody (Cell Signaling Technology). Exposures were 10-30 seconds on Kodak LS film. Quantification was performed by densitometry of exposed films using the NIH Image software.

Results

Vg1 RBP expression during development

Previous work in *Xenopus*, zebrafish and mice indicated that the *Vg1 RBP* gene is expressed in a number of different cell types, including the CNS, migrating neural crest and branchial arches, eye, otic vesicle, pronephros, blood islands, and liver diverticulum (Mueller-Pillasch et al., 1999; Zhang et al., 1999). To begin understanding the role Vg1 RBP plays during embryogenesis, we performed a detailed analysis of its expression pattern, focusing primarily on its expression in the developing nervous system. In stage 17 embryos, just prior to neural fold fusion, *Vg1 RBP* mRNA is expressed throughout the neural plate, in both the superficial and deep layers of the neuroectoderm (Fig. 1A,A′). Although it is not detectable in the surface ectoderm, *Vg1 RBP* mRNA is specifically expressed in the sensorial layer of the epidermal ectoderm, the inner layer of the epidermis that underlies the surface ectoderm (Fig. 1B,B′). This layer of cells surrounds the embryo and gives rise to the placodes, the precursors of several embryonic structures, including the otic vesicle, lens and neural crest (Baker and Bronner-Fraser, 2001). Following neural fold fusion and relumination, strong hybridization is observed throughout the neural tube, with the exception of the ventral floor plate region, which shows little or no expression (Fig. 1B′). At this stage, sensorial layer expression remains strong. In the head region of tailbud stage embryos, there is pronounced expression of *Vg1 RBP* mRNA in the neural tube, otic vesicle, lens and the tips of the neural retina that are in close apposition to the lens (Fig. 1C, and data not shown). In addition, the branchial arches, a target for cranial neural crest migration, are positive for *Vg1 RBP* mRNA expression. Although it is difficult to visualize expression in individual cells in sectioned material, adjacent sections from these embryos show that this same population of cells in the branchial arches also expresses *Xtwist*, a marker for migratory neural crest. Control embryos hybridized with a sense probe were completely negative (data not shown). Thus, *Vg1 RBP* mRNA expression until the tailbud stage is predominantly in the central nervous system, putative neural crest, the sensorial layer of the epidermal ectoderm and their derivatives.

Vg1 RBP AMO cause multiple developmental aberrations

We have made use of AMO to inhibit the translation of *Vg1 RBP* mRNA in embryos and asked how reducing the level of

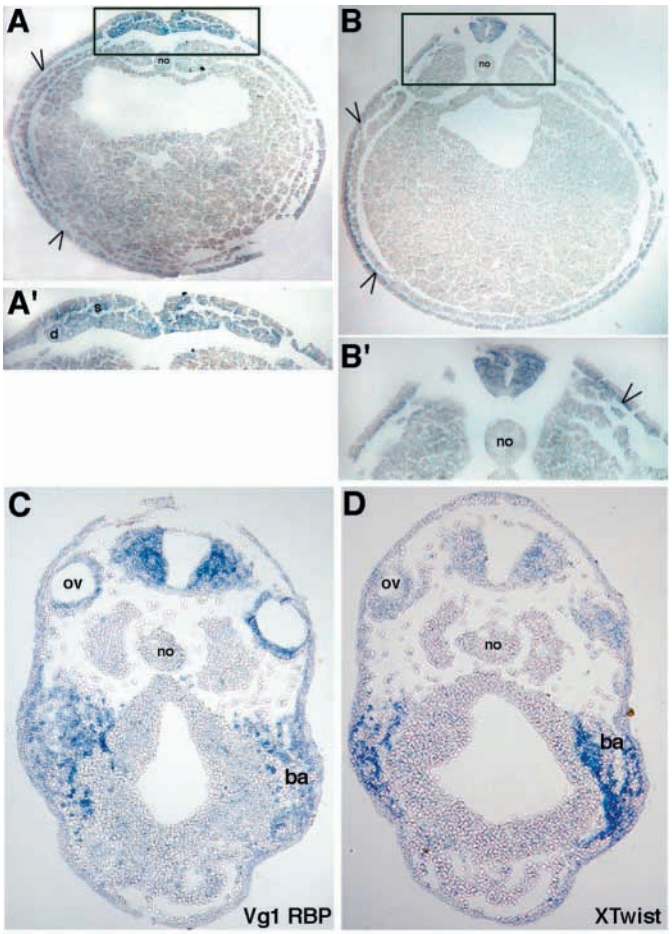

Fig. 1. *Vg1 RBP* mRNA distribution in embryos. Digoxygenin-labeled probes were used to perform in situ hybridization on embryos or sections at different developmental stages. Embryos subjected to whole-mount in situ hybridization (A,A′,B,B′) were embedded in paraffin wax, and transverse sections were analyzed for *Vg1 RBP* mRNA expression. (A,A′) *Vg1 RBP* transcripts are detected throughout the neural plate in stage 17 embryos, including the lateral deep (*d*) layer that contains the prospective neural crest cells and the superficial (*s*) layer, containing the prospective roof plate cells. In addition, the sensorial layer of the epidermal ectoderm is clearly positive for *Vg1 RBP* (open arrowheads). (B,B′) A mid-trunk section of a stage 21 embryo shows that *Vg1 RBP* mRNA is uniformly expressed throughout the closed neural tube. The sensorial layer of the ectoderm remains strongly labeled (open arrowheads). (C,D) Comparison of *Vg1 RBP* and *Xtwist* expression on adjacent sections of a tailbud stage embryo at the cranial levels. (C) *Vg1 RBP* transcripts are detected in the roof plate and throughout the neural tube. In addition, the otic vesicles (ov) and branchial arches (ba) are clearly positive for *Vg1 RBP*. (D) A similar pattern of expression is observed in sections probed for *Xtwist* RNA. *no*, notochord.

the protein affects development. Morpholino oligonucleotides demonstrate a strong affinity to RNA and a marked insensitivity to degradation and have been used successfully to inhibit translation of targeted RNAs (Dibner et al., 2001; Heasman et al., 2000). Both blastomeres of two-cell stage embryos were injected with either control morpholino oligonucleotides (CMO) or AMO, and the embryos were allowed to develop until late tailbud stages. Embryos injected with the control oligonucleotide are essentially indistinguishable from uninjected sibs (Fig. 2A-C). By contrast, injection of the AMO has dramatic and very specific effects on embryonic development (Fig. 2D-F). Antisense-injected embryos show abnormal head morphology, lack lens and dorsal fin, and often display a curved neural tube. In addition, virtually all lateral and ventral pigmentation is absent. As Table 1 shows, this phenotype is highly penetrant, with 95% of antisense-injected embryos showing these abnormalities. By contrast, 97% of embryos injected with CMO have a normal phenotype.

Two lines of evidence suggest that the effects of injecting the AMO are a direct result of interfering with normal Vg1 RBP expression. First, Vg1 RBP translation is reduced fivefold, relative to an internal control, as a result of the AMO injection; CMO have no effect whatsoever on translation of the protein (Fig. 2I). Second, it is possible to rescue the antisense-injected embryos with sense *Vg1 RBP* RNA. Inasmuch as AMO were directed against a site in the 5′ UTR of *Vg1 RBP* mRNA, a *Vg1 RBP* RNA lacking 5′ UTR sequences was synthesized in vitro and injected simultaneously into embryos along with the AMO. These embryos develop normal heads, eyes and pigmentation, and a fairly straight neural tube (Fig. 2G). The rescue is efficient, with 88% of the embryos showing a rescued phenotype, as opposed to 100% mutant phenotypes in the absence of injected sense RNA in these sets of experiments (Table 1). Many of these embryos do show some slight abnormalities posteriorly, suggesting that these may be the result of some non-specific effects of the AMO. Alternatively, the AMO are likely to be more stable than the injected RNA used to rescue the embryos, and therefore their effects may be more pronounced as development proceeds. Significantly, overexpression of sense *Vg1 RBP* mRNA, in the absence of the AMO, has no effect on embryonic development

Table 1. Frequencies of phenotypes obtained from injection experiments

A	WT (*n*)	Mutant phenotype (*n*)	Total number
Uninjected	97% (117)	3% (4)	121
CMO injected	97% (124)	3% (4)	128
AMO injected	5% (8)	95% (140)	148

Frequency of the phenotypes obtained from AMO injection, as compared to sibling, uninjected or CMO-injected embryos. For a definition of the criteria used to define the mutant phenotype, see text.
Six independent experiments were carried out

B	WT/rescued phenotypes (*n*)	Mutant phenotype (*n*)	Total number
Uninjected	90% (44)	10% (5)	49
CMO injected	93% (27)	7% (2)	29
AMO injected	0% (0)	100% (34)	34
AMO+sense RNA injected	88% (29)	12% (4)	33

Coinjection of sense Vg1 RBP RNA with AMO results in the rescue of the mutant phenotypes.
Rescued phenotype, for these experiments, was defined as normal pigmentation, normal head formation, and the presence of normal eyes (see Fig. 2H). Three independent experiments were carried out.

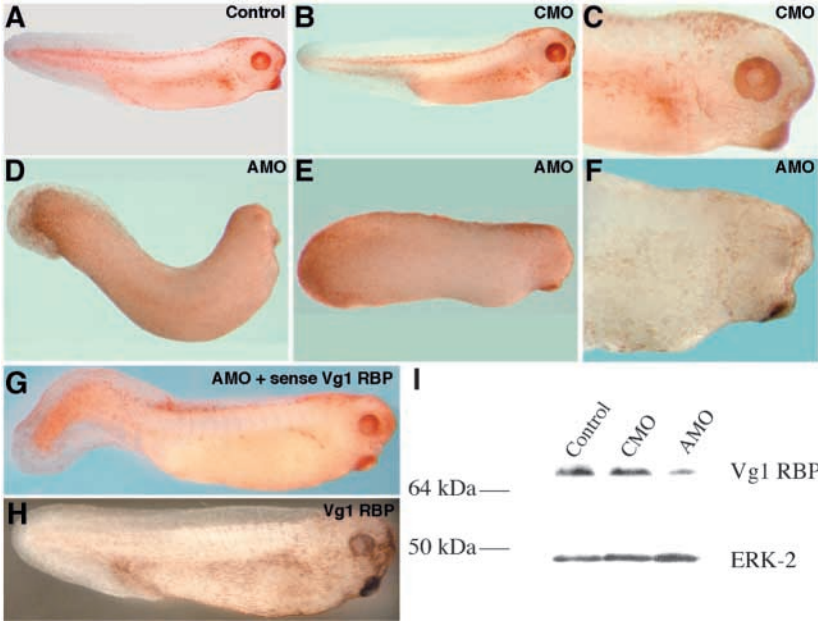

Fig. 2. Specific effect of antisense *Vg1 RBP* oligonucleotide on *Xenopus* development. Two-cell stage embryos were injected in both blastomeres with equal amounts of CMO (B) or AMO (D,E) and allowed to develop to the tailbud stage. Embryos injected with CMO were identical to uninjected sibling embryos (A). Note the abnormal head development, lack of dorsal fin, curved neural tube, and severe reduction in normal pigmentation in embryos injected with AMO. (C,F) Close-up views of the head regions of B and E, respectively, show defective lens formation in the AMO-injected embryos (F). Note the presence, in these embryos, of a pigmented retinal epithelium below the undifferentiated, overlying ectoderm. (G) Sense *Vg1 RBP* mRNA can rescue AMO-injected embryos. Both blastomeres of two-cell stage embryos were co-injected with AMO and sense *Vg1 RBP-GFP* mRNA, lacking the 5′ UTR that contains the AMO target sequence. Embryos were allowed to develop until tailbud stage. Note the rescue of lens and dorsal fin formation and of melanophore migration. (H) Overexpression of *Vg1 RBP-GFP* mRNA alone does not affect the normal development of the embryo. (I) *Vg1 RBP* translation is reduced specifically by AMO injection. Proteins were extracted from tailbud-stage, uninjected (*control*) embryos, and from embryos injected with either CMO (*CMO*) or AMO (*AMO*). Two embryo-equivalents were loaded in each lane and Vg1 RBP expression was analyzed by electrophoresis and western blot analysis using an anti-Vg1 RBP antibody. As measured by densitometry, Vg1 RBP levels are reduced to 20% of original levels in the AMO-injected embryos relative to both uninjected and CMO-injected embryos; samples were normalized to the internal ERK-2 control (detected by anti-ERK-2 antibody).

(Fig. 2H), suggesting that embryos require a crucial, minimal concentration of Vg1 RBP above which development proceeds normally. Overall, the effects of the AMO appear to be highly specific, and indicate a role for Vg1 RBP in several different developmental processes.

To ascertain more precisely the effects of downregulating Vg1 RBP expression in the embryo, we looked at the histology of injected embryos. By injecting a fluorescent nucleo-lipophilic dye into the embryos before first cleavage, which acts essentially as a counterstain, it is possible to image transected, fixed embryos using a confocal microscope (Davidson and Keller, 1999). The cells that form the roof plate of the neural tube migrate, after neural fold fusion, from the lateral part of the superficial neuroectoderm towards the midline, where they narrow and elongate to form the dorsal aspect of the tube; this movement is also thought to lead to a narrowing and elongation of the neural tube (Davidson and Keller, 1999; Linker et al., 2000). In the AMO-injected embryos, the neural tube is open on its dorsal side (Fig. 3B,B′, arrowhead). This lack of a roof plate in the neural tube, even when the overlying ectoderm is fused normally, continues throughout later stages, as observed in both confocal and paraffin wax embedded histological sections (Fig. 3D,F). The neural tube in the AMO-injected embryos also appears to be wider than in control embryos, consistent with a disruption in normal cell movements. Normal roof-plate formation is restored, however, in AMO-injected embryos rescued with sense *Vg1 RBP* mRNA (Fig. 3G).

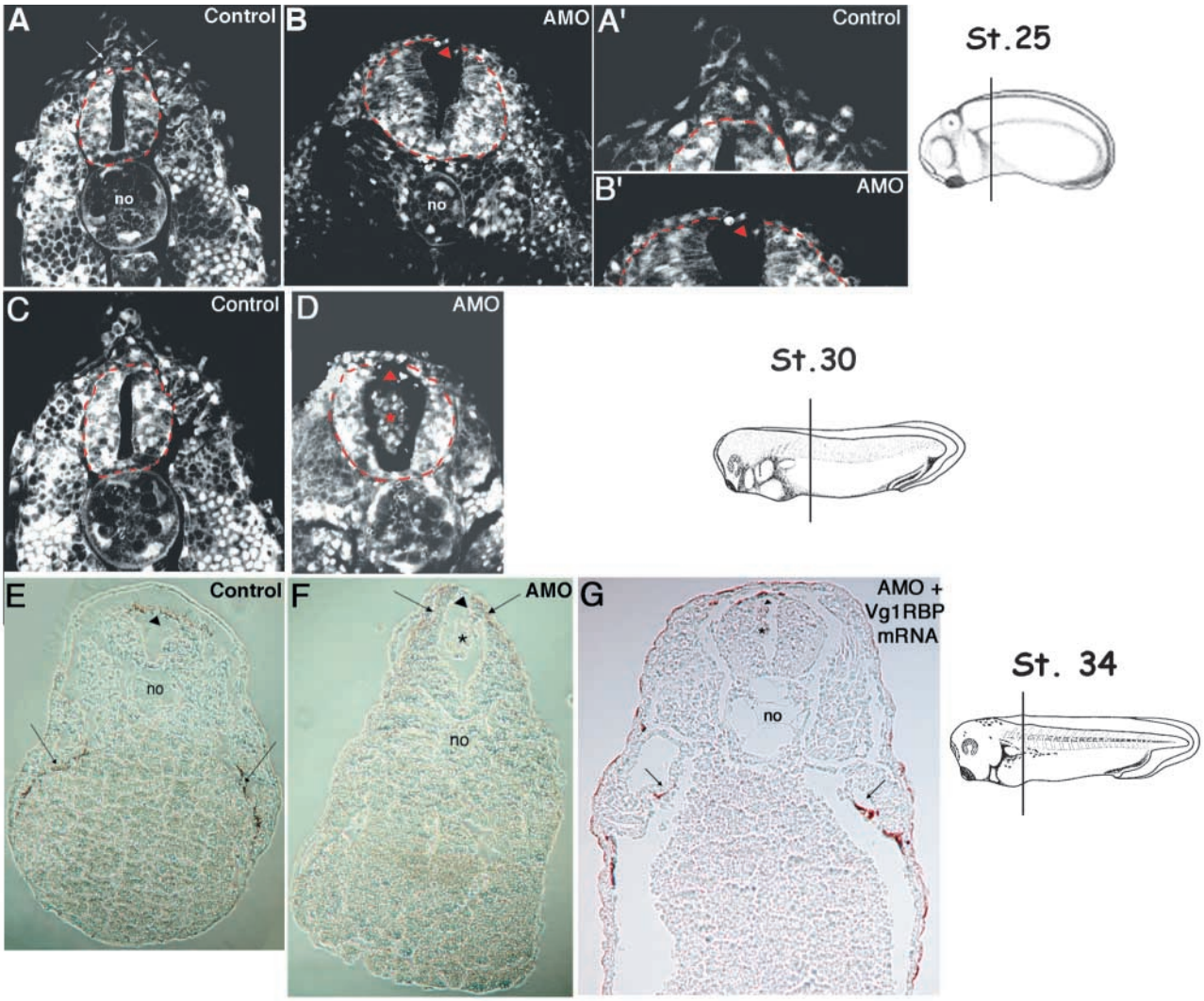

Fig. 3. Antisense *Vg1 RBP* oligonucleotides disrupt roof plate formation and neural crest migration. Transverse confocal and paraffin sections were obtained from tailbud stage embryos injected with CMO (A,A′,C,E), AMO (B,B′,D,F), or AMO with sense *Vg1 RBP* mRNA (G). For each experiment, the approximate plane of section is indicated. Neural crest cells, indicated by the arrows, are found dorsal to the neural tube in CMO-injected embryos (A,A′,C), but are not detectable in the corresponding AMO-injected embryos (B,B′,D). A′ and B′ are high power magnifications of A and B, respectively. By stage 34, pigmented melanophores are observable both above the roof plate and at lateral-ventral positions in embryos injected with either CMO (E), or with AMO and sense *Vg1 RBP* mRNA (G). In AMO-injected embryos at this stage (F), however, the only detectable pigment is in the dorsal half of the neural tube and is completely absent from the lateral or ventral regions. The position of the neural tube roof plate is indicated by an arrowhead; note that it is missing in the AMO-injected embryos (B,B′,D,F), and normally formed in the 'rescued' embryos (G). Apparently apoptotic cells (*) are observed in the lumen of AMO-injected, tailbud stage embryos (D,F,G). In A-D, the neural tube is outlined in red. *no*, notochord.

These data indicate that the migration of roof plate cells to the dorsal midline of the forming neural tube is dependent on Vg1 RBP expression.

The absence, in the AMO-injected embryos (Fig. 2), of lateral and dorsoposterior melanophores, which are derived from neural crest cells, and the lack of a dorsal fin, an epithelial structure that is populated by neural crest, suggested that this highly motile population of cells has also been affected. In stage 25 control embryos, neural crest cells have migrated dorsal to the neural tube and can be observed populating the dorsal fin (Fig. 3A,A′). In the AMO-injected embryos, however, no dorsal fin is formed, and no neural crest cells are detectable (Fig. 3B,B′). A similar phenotype is evident in early tailbud (stage 30) embryos as well (Fig. 3C,D). By stage 34, in control embryos, melanophores (easily detected as the pigmented cells in paraffin sections) can be seen both dorsally, above the roof plate of the neural tube, and laterally, along the flank dorsolateral to the yolky endoderm (Fig. 3E). By contrast, in the AMO-injected embryos, the only observed melanophores have not left the dorsal half of the neural tube, and none are seen along the lateral flank (Fig. 3F). This lack of neural crest migration is observed throughout the AP axis, until the tail region (data not shown). This defect is also corrected by injection of sense *Vg1 RBP* mRNA (Fig. 3G). Thus, neural crest migration along at least two different pathways also requires Vg1 RBP expression.

Cells in the lateral edge of the neural tube are specified correctly, but do not migrate, in AMO-injected embryos

The lateral edges of the neuroectoderm give rise to both roof plate cells, from the superficial layer, and neural crest cells, from the deep layer (Davidson and Keller, 1999; Linker et al., 2000; Schroeder, 1970). The inhibition of cell movements observed upon reduction of Vg1 RBP expression may be the result of interfering with intrinsic cell migration or disrupting normal cell differentiation. To distinguish between these two possibilities, we examined the effects of inhibiting Vg1 RBP translation on the expression of lateral fold markers. *Xpax3*, a paired-domain transcription factor, is expressed in cells that form the roof of the neural tube. Immediately prior to neural fold fusion, it is expressed throughout the neural plate, but after fusion, *Xpax3* expression is detected in a single layer of cells at the dorsal midline of the tube (Bang et al., 1997; Davidson and Keller, 1999). No significant differences in either the level or pattern of *Xpax3* expression are detected in CMO- when compared with AMO-injected embryos, at early neurula stages (Fig. 4A,C). After neural fold fusion, the level of *Xpax3* expression remains unchanged in both CMO- and AMO-injected embryos; however, a clear difference in the pattern of its expression is observed. In CMO-injected embryos, *Xpax3* is expressed in a single stripe along the dorsal midline (Fig. 4B), whereas in AMO-injected embryos, a conspicuous medial groove devoid of *Xpax3* expression is present (Fig. 4D). These results indicate that although the prospective roof-plate cells are properly specified, their medial migration is prevented by the injection of AMO.

As markers for neural crest specification, we monitored the expression of the transcription factors *Xsnail* and *Xtwist* (Essex et al., 1993; Hopwood et al., 1989; Sargent and Bennett, 1990). *Xsnail* is expressed in the deep layer of the lateral edges of the neuroectoderm, where neural crest cells

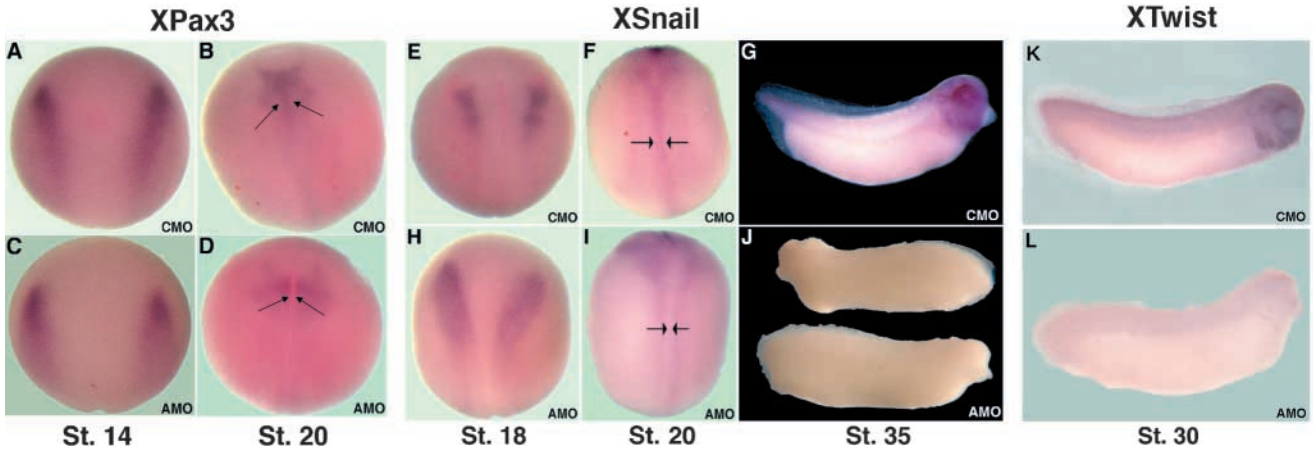

Fig. 4. Downregulation of Vg1 RBP does not affect roof plate and neural crest cell determination. *Xpax3* mRNA expression was assayed by in situ hybridization, in embryos injected with either CMO (A,B) or AMO (C,D). Dorsal view of a CMO- (A) and AMO- (C) injected embryos at stage 14 showing expression of *Xpax3* in the lateral domains of the neural plate. Following neural fold fusion, in CMO-injected embryos (B), roof-plate cells normally reach the midline and *Xpax3* expression is observed in the dorsal aspect of the tube (arrows). In AMO-injected embryos (D), roof plate cells fail to migrate medially, and a groove devoid of *Xpax3* expression is observed along the dorsal midline (arrows). *Xsnail* expression was also analyzed in CMO- (E-G) and AMO- (H-J) injected embryos. In stage 18 embryos, immediately preceding neural fold fusion, expression of *Xsnail* is not reduced, and in fact is somewhat enhanced, by AMO injection (H) when compared with embryos injected with CMO (E). After neural fold fusion, *Xsnail*-expressing cells are observed along the dorsal midline (arrows) in the CMO-injected embryos (F). In AMO-injected embryos at the same stage (stage 20; I), however, *Xsnail* expression is absent from the dorsal midline and instead is observed flanking the midline on either side (arrows). In stage 35 embryos injected with CMO, cells continue to express *Xsnail* in the branchial arches and throughout the head region (G), whereas no expression of *Xsnail* is detected anywhere in AMO-injected embryos at the same stage (J). (K,L) *Xtwist* expression in injected embryos. As seen with *Xsnail*, a dramatic reduction in the expression of the cranial neural crest marker *Xtwist* is observed in stage 30 embryos injected with AMO (L) when compared with the sibling CMO-injected (K) embryos. A-F,H,I are dorsal views; G,J,K,L are lateral views.

originate, and continues to be expressed in prospective cranial and trunk neural crest from mid- to late neurula stages and in migratory and post-migratory neural crest in tailbud and later stages (Linker et al., 2000). *Xtwist* expression begins somewhat later than that of *Xsnail*, appearing in the cranial neural folds at stage 16, and is observed in migratory cranial, but not trunk, neural crest in stages 25-30 (Linker et al., 2000). The expression of *Xsnail* in pre-migratory neural crest, observed at the lateral borders of the anterior neural plate, is not downregulated by AMO injection; in fact, there appears to be a slight broadening of the expressing regions (Fig. 4E,H). After neural tube closure, *Xsnail*-positive neural crest cells, which migrate medially to the dorsal midline (Fig. 4F), exit the neural epithelium and begin to migrate along pathways determined by their position along the AP axis. Normally, by stage 24-25, *Xsnail*-positive neural crest cells have begun to populate all of the branchial arches, and *Xsnail* expression is observed in the post-migratory cranial neural crest for at least an additional day (Fig. 4G). In the antisense-injected embryos, however, no *Xsnail*-expressing cells are detectable in the head at all; indeed, all *Xsnail* expression disappears from the embryo beginning at stage 24 onwards (Fig. 4J, and data not shown). *Xtwist*-expressing cells, normally present in the branchial arches of stage 30 embryos (Fig. 4K) are also absent from the AMO-injected embryos (Fig. 4L). A similar disappearance of neural crest markers has been observed in embryos in which neural crest migration has been inhibited by overexpression of a cadherin molecule (Borchers et al., 2001). These results show that neural crest determination appears to proceed normally in the antisense-injected embryos until the stage at which, in control-injected embryos, neural crest begin to migrate and exit the neural tube. Thus, inhibition of Vg1 RBP expression prevents the movement of *Xsnail* and *Xtwist*-expressing neural crest cells.

Xsnail is also expressed in the prospective roof plate cells in the superficial layer of the lateral edge of the neural plate, from mid-neurula stages (Essex et al., 1993; Linker et al., 2000). After neural fold fusion, these cells continue to express *Xsnail* at the midline in the CMO-injected embryos (Fig. 4F, arrows). In AMO-injected embryos after neural fold fusion, however, the medial population of *Xsnail*-expressing cells is completely absent (Fig. 4I, arrows); instead, as seen with the *Xpax3* expression, there are two stripes of expressing cells that can be observed adjacent to the dorsal midline. These results reinforce the conclusion from the histological analysis that the neural tube in these embryos is open on its dorsal side (Fig. 3B,D, arrowhead).

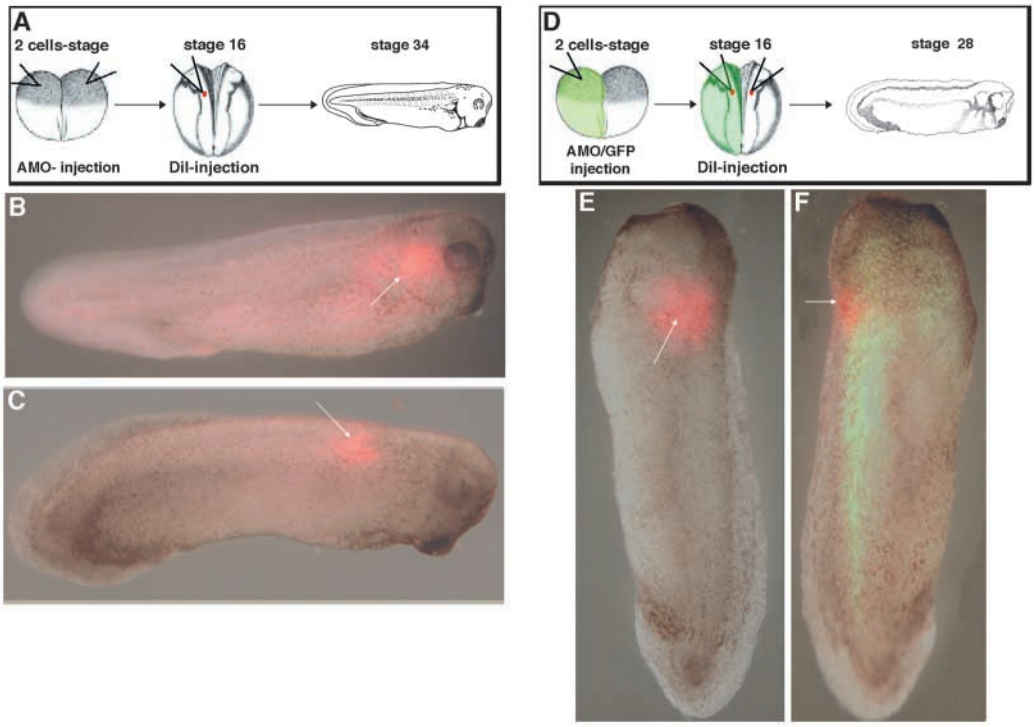

Fig. 5. AMO-injected embryos show inhibition of DiI-labeled neural crest migration. Both blastomeres of two-cell stage embryos were injected with AMO, allowed to develop to stage 16, and then injected with the lipophilic dye DiI into the dorsal neural folds in the area of the hindbrain, containing presumptive cranial neural crest cells (A). Upon reaching stage 34, the embryos were examined under a fluorescent stereoscope. (B) In control embryos injected only with DiI, fluorescent cells are observed around the branchial arches (arrow), a target for cranial neural crest cells (in 44/51=86% of embryos). By contrast, in AMO-injected embryos (C), DiI-labeled crest cells remain in the dorsal aspect of the neural tube (arrow; in 31/43=72% of embryos; n=3). In a different set of experiments (D), a single blastomere of two-cell stage embryos was injected with AMO along with *GFP* RNA, used as a lineage tracer. Embryos were allowed to develop to stage 16 and were then injected with DiI on both the right and left sides of the dorsal neural folds, in the same area of the hindbrain as in A. Upon reaching stage 28, embryos were examined under a fluorescent stereoscope. On the untreated side (E), streams of cells (arrow) migrating from the site of injection ventrally, towards the branchial arches, are observed (in 68/68=100% of embryos). On the AMO/GFP-treated side (F), DiI-labeled cells are observed above the neural tube (arrow), and no fluorescence is detected in or around the branchial arches (in 49/68=72% of embryos; n=3).

Cranial neural crest do not migrate in AMO-injected embryos

Cranial neural crest cells originate at the lateral edges of the neural plate, in the midbrain-hindbrain region, prior to neural fold fusion, and migrate along three distinct pathways: mandibular, hyoid and branchial (Mayor et al., 1999). We followed directly the migration along the branchial pathway of the cranial neural crest cells by labeling the lateral edge of the neural plate, in the posterior part of the rhombencephalon, with the hydrophobic dye DiI (Collazo et al., 1993) (Fig. 5A). Embryos injected with AMO in both blastomeres of a two-cell embryo were labeled at stage 16 and allowed to grow until stage 34, when they were fixed and examined under a fluorescence stereoscope. As seen in Fig. 5B, in control embryos, the DiI-labeled cells leave the neural tube and stream towards the branchial arches. In AMO-injected embryos, however, no movement of the DiI-labeled cells is detected (Fig. 5C). Thus, as suggested by the absence of *Xtwist*-positive cells in the branchial arches of AMO-injected embryos (Fig. 4L), downregulation of Vg1 RBP inhibits cranial neural crest migration in embryos.

The inhibition of cranial neural crest migration could be the result of either global inhibitory mechanisms, such as defective neural tube formation and/or a general toxicity, or more localized effects, resulting from an interference with mechanisms intrinsic to the affected cells and their immediate environment. To distinguish between these two possibilities, we injected a single blastomere at the two-cell stage with both AMO and an mRNA encoding GFP, and then, at stage 16, bilaterally labeled the lateral edges of the neural plate at the level of the posterior hindbrain (Fig. 5D). Embryos were fixed at stage 28 and examined, as above, by fluorescence stereo-microscopy. On the control side of the embryo, DiI-labeled cells are clearly detected migrating towards the branchial arches (Fig. 5E). On the AMO/*GFP*-injected side of the same embryos, however, the cells remain along the dorsal midline and no fluorescence is observed outside of the neural tube (Fig. 5F). These results show that AMO prevent neural crest migration even when contralateral neural crest, at the same AP axial level, migrate normally, strongly suggesting that the inhibition of migration is mediated locally, rather than globally.

AMO-mediated inhibition of neural crest migration is not dependent on an open neural tube

Medial migration of the cells forming the roof plate of the neural tube occurs in stage 16-17 embryos, in conjunction with, although faster than, neural crest migration towards the midline (Linker et al., 2000). Given the absence of a closed neural tube in the AMO-injected embryos, it is formally possible that the inhibition of neural crest migration in these embryos may be a consequence of faulty roof-plate formation, and not a result of interference with an intrinsic cell motility mechanism. To distinguish between these options, we have generated embryos with a milder phenotype by injecting a lower concentration of AMO. These embryos develop normal eyes, and the overall morphology of the embryo appears normal as well. In fact, as revealed in cross-sections of these embryos taken from two different stages, the neural tube is closed and even appears to attain a normal width by stage 30 (Fig. 6B,D). Nevertheless, few if any neural crest cells are present above the neural tube or in the dorsal fin region, as are seen in control embryos examined at the same AP levels (Fig. 6A,C). Thus, neural crest and roof plate cell migration appear to be independent events, the inhibition of which is differentially dependent on AMO concentration.

Vg1 RBP is localized to processes of migratory neural crest and is required for outgrowth

Given that neural crest migration is inhibited by reduced Vg1 RBP expression, we decided to examine Vg1 RBP intracellular distribution in cultures of migrating neural crest cells. Neural primordia containing premigratory neural crest were excised from stage 20-22 embryos and allowed to attach to fibronectin-coated surfaces (Fig. 7A). After an overnight incubation, neural crest cells migrated out of the intact neural tubes onto the

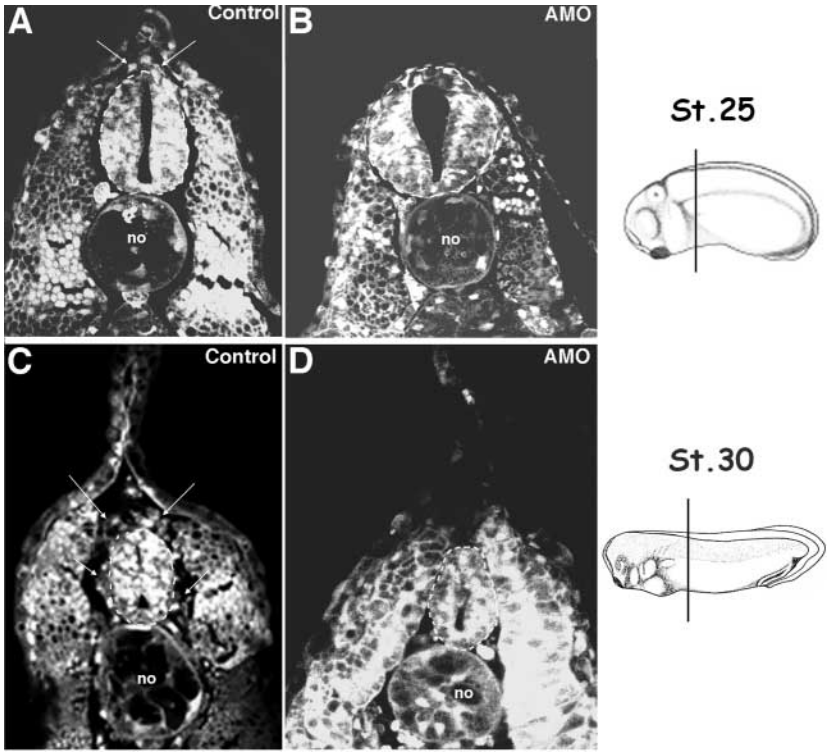

Fig. 6. Inhibition of neural crest migration in AMO-injected embryos is independent of neural tube closure. Two-cell stage embryos injected in both blastomeres with a low concentration (6.5 ng/blastomere) of AMO (B,D) were analyzed by confocal microscopy for neural crest cell migration and neural tube closure, when compared with uninjected controls (A,C). In stage 25 control embryos, neural crest cells (arrows) can be observed above the neural tube (A), but are completely absent in AMO-injected embryos (B). By stage 30, in control embryos (C), migrating neural crest cells move ventrally around the neural tube, as well as into the dorsal fin. In sibling, AMO-injected embryos (D), no migrating neural crest cells are detected. Note the completely sealed neural tube in the AMO-injected embryos; the neural tube is outlined in white. *no*, notochord.

substrate. Immunolabeling of the HNK-1 epitope, that characterizes migratory neural crest cells in avian species (Lim et al., 1987), revealed the presence of multipolar mesenchymal cells, as well as neurons with round cell bodies that contained one or two processes (Fig. 7D). In addition, many melanophores were present [whose pigment masks antibody reactivity (Fig. 7B,C)]. We estimate that at least 90% of the emigrating cells are neural crest derivatives (i.e. either HNK-1 positive or melanophores). Vg1 RBP expression is detected in a large majority of the emigrating cells (Fig. 7E,F). Strikingly, this expression is observed to be asymmetric in 77% of the cells, with particularly strong fluorescence detectable in the long processes present on many of the cells (Fig. 7G-I). These processes are also generally oriented distally away from the explanted tube. The neural tube remains strongly Vg1 RBP positive, even after many of the neural crest cells have exited, suggesting that Vg1 RBP is likely to be expressed also in other cells deriving from the neuroectoderm. Although we were unable to stain for both HNK-1 and Vg1 RBP simultaneously, because of the different fixation techniques required for each ligand, it is clear from its broad expression pattern that Vg1 RBP protein is present in most, if not all, explanted neural crest cells, and its distribution is associated with extended protrusions at the distal edge of the migrating cells.

To further examine the effects of Vg1 RBP inhibition, we assayed neural crest migration from neural tubes explanted from AMO-injected embryos. In all of these cases, neural crest outgrowth was either completely inhibited or severely impaired (Fig. 7K). To quantify this difference, we arbitrarily defined a region of 15 μm surrounding the explant and counted the cells that migrated beyond this area. A dramatic drop was observed in the number of neural crest cells migrating out of the AMO explants (21±13.7, n=3) as compared to those exiting the normal neural tube explants (136±17, n=3). Those neural crest cells that do migrate out of the explant express Vg1 RBP (Fig. 7L), suggesting that these cells have escaped the AMO-mediated down regulation of Vg1 RBP. Thus, Vg1 RBP inhibition affects neural crest migration both in vivo and in explants.

Discussion

Asymmetric intracellular distributions of VICKZ proteins have been reported in a number of different cell types (Farina et al., 2003; Mori et al., 2001; Nielsen et al., 1999; Oleynikov and Singer, 2003; Zhang et al., 2001a). Here, we show that Vg1 RBP is localized in migrating neural crest cells and that it is required for their movement in the developing *Xenopus* embryo. Roof-plate cell migration is also dependent on Vg1 RBP expression. In light of these results, we suggest that the requirement of this RNA binding protein in cell migration is likely to be dependent on its subcellular localization.

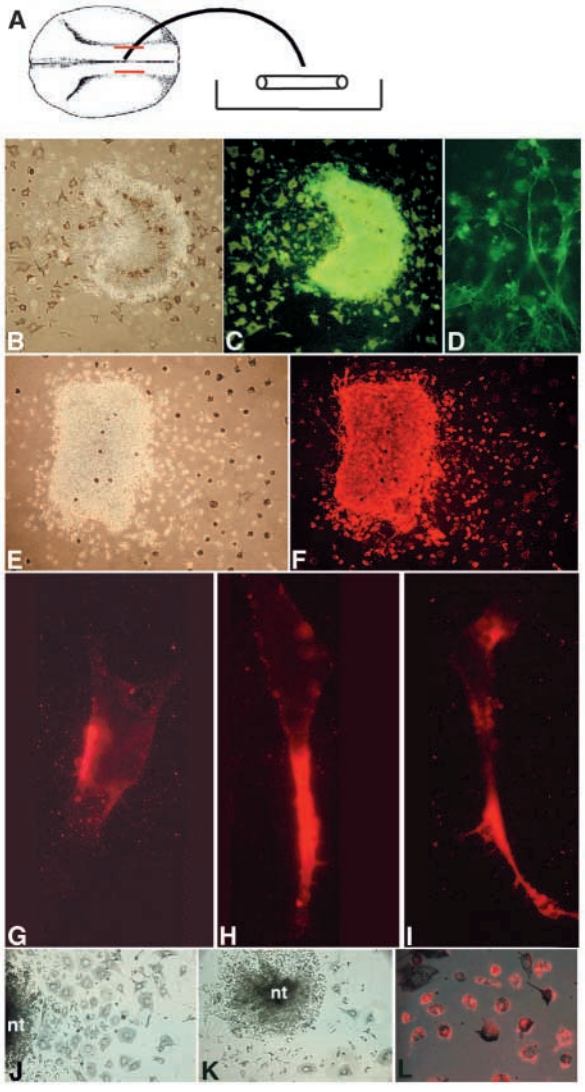

Fig. 7. Vg1 RBP is asymmetrically localized in explanted neural crest cells and required for their migration. Stage 20-22 embryos were cut horizontally in the middle of the embryo, and a caudal piece of trunk neural tube (indicated schematically by red lines in A) containing premigratory neural crest cells was placed in a petri dish coated with fibronectin. Twenty-four hours of incubation at 25°C led to an emigration of up to several hundred cells, with several different morphologies. Generally, the tubes rolled onto their sides, leading to an asymmetric outgrowth of the neural crest on one side of the explanted tube. (B) Phase-contrast image; (C) the fluorescence micrograph of an explanted neural tube stained with the anti-HNK1 antibody. (D) Emigrating neural crest cells and neural fibers stain positive for HNK1. (E,F) Explanted neural tube and outgrowing cells were stained with anti-Vg1 RBP antibody and viewed using phase-contrast (E) or fluorescence (F) microscopy. For both the anti-HNK1 and anti-Vg1 RBP antibodies, note the fluorescence in the neural tube and in the majority of the cells that have migrated out of the tube. (Melanophores, because of their pigment, do not show noticeable fluorescence.) (G-I) Representative patterns of asymmetric distribution of Vg1 RBP in migratory neural crest cells. Vg1 RBP is observed at different sites in neural crest cells, including along the membrane (G), and in processes that generally point away from the explanted tissue (H,I). (J-L) Injection of AMO reduces the migration of neural crest cells in explants. Neural tubes from stage 20-22 embryos, injected with either CMO (J) or AMO (K), were cultured as described in A. The number of cells that migrate out of the explant from AMO-injected embryos (K) was reduced approximately threefold when compared with that from CMO-injected embryos (J). Immunostaining of the AMO-injected explants shows that these migrating cells are positive for Vg1 RBP (L). Note the presence of differentiated neural crest derivatives in the explant cultures, suggesting that both the cells and the tube remained viable during the course of the assay.

Specificity of AMO-induced phenotypes

Several lines of evidence indicate that the AMO-injection phenotypes are a direct result of inhibiting Vg1 RBP expression, and not the result of a non-specific toxic effect. First, Vg1 RBP protein level is reduced fivefold, relative to an internal control, in the AMO-injected embryos. Second, *Vg1 RBP* mRNA, engineered not to be a target for the AMO, rescues these embryos when injected in parallel with the AMO. Third, the AMO appears to function in a dose-dependent fashion. At lower concentrations, neural crest migration is predominantly affected, while lens and neural tube formation appear normal. Higher concentrations of AMO lead to abnormal tube formation and the absence of a lens and dorsal fin. Fourth, when only one of two blastomeres at the two-cell stage is injected with AMO, migration on the uninjected side is normal. Fifth, all of the sites affected by AMO injection are tissues where Vg1 RBP is normally expressed. Taken together, these results argue strongly that the reduction of Vg1 RBP protein levels leads to specific, pleiotypic phenotypes.

Two *Vg1 RBP* cDNAs have been described in *Xenopus laevis*, originally termed *Vg1 RBP D* and *B* (Havin et al., 1998), encoding proteins that are 97% identical. *Vg1 RBP D* is identical to *Vera*, a *Vg1* RNA-binding protein described previously (Deshler et al., 1998), and *Vg1 RBP A* is identical to a protein in GenBank called B3, which was isolated on the basis of its ability to bind a DNA element upstream to the gene *TFIIIA* (Griffin et al., 2003). Given the pseudotetraploid nature of *Xenopus laevis*, it seems likely that these cDNAs represent two alleles of the same gene rather than independent genetic loci. In higher vertebrates, the three distinct *VICKZ* genes reside on three separate chromosomes (Yaniv and Yisraeli, 2002). In *Xenopus laevis*, we (Havin et al., 1998) and others (Mueller-Pillasch et al., 1999) have not found evidence of any additional VICKZ proteins. The antisense morpholino oligonucleotide used in these studies was directed against the 5′ UTR of *Vg1 RBP D* in a region that is not homologous to *Vg1 RBP A*. Thus, the phenotypes reported here can be attributed directly to the reduced expression of a single gene, *Vg1 RBP D*.

Role of Vg1 RBP in roof plate and neural crest movements

The initial stages of determination of both presumptive roof plate and neural crest cells are unaffected by the AMO injection. The presence of melanophores dorsal to the neural tube (Fig. 3), even in the antisense-injected embryos, suggests that Vg1 RBP is not required for the initial specification of neural crest cells, but rather is necessary for their migration. In addition, cells expressing *Xpax3* and *Xsnail* continue to express these markers in the AMO-injected embryos for some period of time after migration has commenced in parallel CMO-injected sibs (see Fig. 4, and data not shown), indicating that these cells are still viable, even if sessile. Indeed, the slightly broader domain of *Xsnail* expression, as well as the wider neural tube, observed in the AMO-injected embryos (Fig. 3) may also reflect the inhibited migration of cells located at the lateral edge of the neuroectoderm.

After 24 hours, all *Xsnail* and *Xtwist* expression has disappeared from the AMO-injected embryos, while the CMO-injected embryos display the normal neural crest staining pattern. Loss of *Xsnail* and *Xtwist*-positive cells in AMO-injected embryos could be the result of either death of the non-migrating cells or downregulation, perhaps coupled with transdetermination, of the sessile cells. The fact that roughly equal amounts of DiI-labeled neural crest cells are maintained in both antisense and control-injected embryos, despite the lack of movement of these cells in the former case, suggests that certainly massive cell death is not occurring. In the case of neural crest cells whose migration was inhibited by the overexpression of either full length Xcadherin 11 (Xcad-11) or Xcad-11 lacking its cytoplasmic domain, neural crest markers such as *Xsnail* and *Xtwist* were downregulated after 4 hours, and completely lost after 18 hours; neural markers, however, such as *N-tubulin* and *nrp-1*, were activated during this same period in the non-migrating cells (Borchers et al., 2001). Our results are consistent with such a reprogramming of neural crest, although we cannot exclude the possibility that blocking migration may eventually lead to a small increase in cell death. By stage 34, cross-sections of AMO-injected embryos show some cells present in the lumen of the neural tube (not seen in control embryos) that are likely to become apoptotic (Fig. 3D,F,G). Such cells are not seen at earlier stages in the AMO-injected embryos (Fig. 3B), even in stages at which control embryos contain migratory neural crest. Thus, if AMO-injection does eventually lead to some apoptosis, it occurs considerably after the block in migration.

Despite the fact that AMO-injection inhibits both roof plate formation and neural crest migration, it appears that one event is not dependent upon the other. Neural crest migration can proceed normally even in the presence of an open neural tube (Regnier et al., 2002) (C.K., unpublished). In embryos injected with a low concentration of AMO, the neural tube is closed, but, nevertheless, neural crest migration is inhibited (Fig. 6). Taken together, these data suggest that the formation of the neural tube roof plate and the migration of neural crest out of the tube are independent events that both require Vg1 RBP expression.

It is interesting to speculate as to how and why the roof plate and neural crest cells respond differently to low concentrations of AMO. We note that the high concentration of AMO used in this study reduced the overall level of Vg1 RBP expression to 20% of wild-type levels, but did not eliminate it completely. [This may be the result of large, excess amounts of Vg1 RBP present in cells; we estimate that there is at least a 100-fold molar excess in oocytes of Vg1 RBP over *Vg1* mRNA (JKY, personal observations). This excess may also explain why no effect is observed when Vg1 RBP is overexpressed in embryos (Fig. 2H).] It is unclear whether the 20% expression of Vg1 RBP reflects a lower level in all cells or a mosaic expression. The fact that the few cells managing to migrate out of neural tube explants taken from AMO-injected embryos are Vg1 RBP-positive may be indicative of such a mosaic pattern. Perhaps, in embryos injected with a low concentration of AMO, those cells that need to migrate only a small distance (such as roof plate cells) may express the minimal amount of Vg1 RBP necessary for migration. Those cells requiring longer distances of migration (such as neural crest cells) may not have the levels necessary for persistent, extended movement. Alternatively, only a few roof plate cells may be required to reach the midline in order to close the neural tube. Studies aimed at modulating the levels of Vg1 RBP in cells should help in understanding how Vg1 RBP functions.

Vg1RBP mediates specific types of cell movement

Different types of cell movements are required for normal embryonic development (Locascio and Nieto, 2001). Convergent-extension facilitates gastrulation, and these integrative, tissue movements appear to exhibit planar-cell polarity (Wallingford et al., 2000). Inhibition of the non-canonical Wnt signaling pathway prevents both gastrulation and neurulation movements, including neural fold fusion of the ectoderm (Goto and Keller, 2002; Wallingford and Harland, 2001; Wallingford and Harland, 2002). In the AMO-injected embryos, however, both gastrulation and neural fold fusion occur normally. It is the migration of individual neural crest and roof plate cells, both of which appear to exhibit a monopolar, protrusive movement, that is inhibited and, in the latter case, that results in a neural tube that is open on its dorsal side. These data suggest that different mechanisms orchestrate individual cell movements, as opposed to integrative, tissue behavior, in various tissues.

Davidson and Keller (Davidson and Keller, 1999) have shown, using time-lapse fluorescence microscopy, that the cells forming the dorsal neural tube exhibit a protrusive migration towards the midline from the lateral margins of the neural plate. These cells have apparently already undergone an epithelial-to-mesenchymal transition (EMT) in order to migrate as individual cells. It is these *Xpax3*-positive cells that fail to achieve their dorsal midline localization in the AMO-injected embryos (Fig. 4D). The monopolar morphology of these cells is very similar to both that observed by these researchers in neural crest cells migrating from the lateral edges underneath the overlying epidermis towards the midline (Davidson and Keller, 1999), and that which we observe in neural crest migrating out of the neural tube explant in culture (Fig. 7). Although it is difficult to determine the direction of migration of a given cell in a static picture, the protein accumulates, in a large majority of the cells, in what appear to be processes pointing away from the explanted tube. It is tempting to speculate that Vg1RBP is required in the polar processes for proper migration in all of these cells, after they have undergone EMT. This localization is reminiscent of the subcellular distribution reported for some of the VICKZ proteins in different cell types (Farina et al., 2003; Nielsen et al., 2002; Oleynikov and Singer, 2003; Zhang et al., 2001a). Future experiments that mislocalize the protein within the cell will be helpful in determining whether intracellular localization of Vg1 RBP is required for its function.

Mechanism of Vg1 RBP action

Neural crest migration and differentiation involves concerted changes in cell and matrix adhesion, cytoskeletal organization and gene expression. Over the past few years, several molecules have been identified in *Xenopus* embryos, which are involved in these different processes (Alfandari et al., 2001; Bellmeyer et al., 2003; Borchers et al., 2001; Carl et al., 1999; Helbling et al., 1998; Krull et al., 1997; Smith et al., 1997; Wang and Anderson, 1997). Vg1 RBP represents a novel type of molecule, an RNA-binding protein, involved in the process of neural crest migration. Vg1 RBP also plays a role in additional migration events, such as the movement of roof plate cells towards the midline. Given its asymmetric localization in migrating neural crest, and its multiple RNA binding sites, Vg1 RBP could mediate the sorting of certain RNAs required at the leading edge of migrating cells. Any RNA encoding a protein required in large amounts in order to facilitate the rapid formation of new cell membranes or sub-membrane structures would be a potential candidate. Such RNAs might encode extracellular receptors, membrane components, adhesion molecules, β-actin and other cytoskeletal components. Other members of the VICKZ family have been identified as repressing translation or stabilizing mRNAs. These functions may also be important aspects of Vg1 RBPs actions, potentially coupling localization (and perhaps stabilization) of RNA with restricted, intracellular expression. It is formally possible that Vg1 RBPs role in motility is independent of its RNA-binding ability. Experiments in chick embryonic neurons, however, using antisense oligonucleotides directed against the cis-acting localization elements in *β-actin* mRNA, indicate that RNA binding is required for localization of ZBP-1 into neurites and growth cones (Zhang et al., 2001a) and lamellapodia (Oleynikov and Singer, 2003). In addition, Farina and Singer (Farina and Singer, 2003) have recently shown that transfection of certain constructs of ZBP-1 into chick embryo fibroblasts can disrupt both *β-actin* mRNA localization and fibroblast motility. Taken together, these results suggest that Vg1 RBP is likely to be required in neural crest and roof plate cell migration because it facilitates the localization of certain mRNAs to the leading edge of the cell.

This mechanism suggests that Vg1 RBP should function in a cell-autonomous manner. Its expression pattern is consistent with this hypothesis, inasmuch as AMO phenotypes are observed only in tissues in which Vg1 RBP is expressed. In addition, the results from labeling small populations of prospective neural crest in embryos in which Vg1 RBP has been depleted from half of the embryo (Fig. 5) indicate that Vg1 RBP appears to be functioning locally, and not globally. Despite the fact that in neural tubes explanted from AMO-injected embryos, the only neural crest cells that manage to migrate are those that still express Vg1 RBP, further experiments are still required to definitively establish whether Vg1 RBP functions exclusively in a cell-autonomous fashion.

Expression of VICKZ proteins in neoplastic cells

Numerous studies over the last three years have revealed that VICKZ proteins are overexpressed in a wide variety of tumors (reviewed by Yaniv and Yisraeli, 2002). Many individuals with colorectal adenocarcinomas and hepatocellular carcinomas generate antisera against one or more of the VICKZ proteins (Zhang et al., 2001b); in human breast cancers, the gene for the VICKZ protein CRD-BP/IMP-1 is amplified up to 40 times (Doyle et al., 2000). RT-PCR and immunoblotting have shown that *CRD-BP/IMP-1* are expressed in 81% of colorectal carcinomas, 73% of malignant mesenchymal tumors and 14/14 Ewing sarcomas that were examined; strikingly, normal tissues are almost always negative for these genes (Ioannidis et al., 2001; Ross et al., 2001). *p62* (the splice variant of *IMP2*) is detected in all of the malignant cells in 33% of cancer nodules from hepatocellular carcinomas that were examined in one study, but is completely undetectable in adjacent, non-malignant cells and in normal livers (Lu et al., 2001). The results presented here, analyzing for the first time the effects of reducing VICKZ protein expression, raise an intriguing, possible role for these RNA binding proteins in carcinogenesis. In addition to the activation of proteins important for

invasiveness and migration, the expression of VICKZ proteins may be one of many changes required to make neoplastic cells motile, and therefore, a putatively important marker for metastatic potential. It is interesting to note that another gene found to be required for neural crest migration, *snail*, appears to play an important role in the epithelial-to-mesenchymal transition associated with metastasis (Batlle et al., 2000; Blanco et al., 2002; Cano et al., 2000). These results emphasize the close relationship between mechanisms mediating and controlling cell movements in embryos and in neoplasias, and therefore it is perhaps not surprising that similar molecules appear to participate in both of these processes.

We greatly appreciate the advice and assistance of Lance Davidson and Ray Keller in showing us how to make optical sections and helping us understand how neural crest and roof plate cells move in *Xenopus*. Our thanks go to Anna Git for the Vg1 RBP-GFP construct, Avihu Klar for the ERK-2 antibody and Zeev Paroush for his instructive comments on the manuscript. Very special thanks go to Yuval Cinnamon for his invaluable assistance in helping us prepare the figures, and to Froma Oberman for help in editing the text. We would also like to acknowledge the advice and assistance of the Fainsod, Kalcheim and Yisraeli laboratories. K.Y. is supported in part from a Golda Meir Foundation Fellowship and from the Hebrew University Rector's Fellowship for Excellence. Different parts of this project were supported by grants from the Israel Science Foundation (J.K.Y.), Israel Cancer Research Fund (J.K.Y. and C.K.), the US-Israel Bi-National Science Foundation (J.K.Y.), the March of Dimes Birth Defects Foundation (C.K.), and the Deutcheforschungsgemeinschaft (SFB 488; C.K.).

References

Alfandari, D., Cousin, H., Gaultier, A., Smith, K., White, J. M., Darribere, T. and DeSimone, D. W. (2001). Xenopus ADAM 13 is a metalloprotease required for cranial neural crest-cell migration. *Curr. Biol.* **11**, 918-930.

Baker, C. V. and Bronner-Fraser, M. (2001). Vertebrate cranial placodes I. Embryonic induction. *Dev. Biol.* **232**, 1-61.

Bang, A. G., Papalopulu, N., Kintner, C. and Goulding, M. D. (1997). Expression of Pax-3 is initiated in the early neural plate by posteriorizing signals produced by the organizer and by posterior non-axial mesoderm. *Development* **124**, 2075-2085.

Batlle, E., Sancho, E., Franci, C., Dominguez, D., Monfar, M., Baulida, J. and Garcia de Herreros, A. (2000). The transcription factor snail is a repressor of E-cadherin gene expression in epithelial tumour cells. *Nat. Cell Biol.* **2**, 84-89.

Bellmeyer, A., Krase, J., Lindgren, J. and LaBonne, C. (2003). The protooncogene c-Myc is an essential regulator of neural crest formation in Xenopus. *Dev. Cell* **4**, 827-839.

Blanco, M. J., Moreno-Bueno, G., Sarrio, D., Locascio, A., Cano, A., Palacios, J. and Nieto, M. A. (2002). Correlation of Snail expression with histological grade and lymph node status in breast carcinomas. *Oncogene* **21**, 3241-3246.

Borchers, A., David, R. and Wedlich, D. (2001). Xenopus cadherin-11 restrains cranial neural crest migration and influences neural crest specification. *Development* **128**, 3049-3060.

Bubunenko, M., Kress, T. L., Vempati, U. D., Mowry, K. L. and King, M. L. (2002). A consensus RNA signal that directs germ layer determinants to the vegetal cortex of Xenopus oocytes. *Dev. Biol.* **248**, 82-92.

Butler, K., Zorn, A. M. and Gurdon, J. B. (2001). Nonradioactive in situ hybridization to xenopus tissue sections. *Methods* **23**, 303-312.

Cano, A., Perez-Moreno, M. A., Rodrigo, I., Locascio, A., Blanco, M. J., del Barrio, M. G., Portillo, F. and Nieto, M. A. (2000). The transcription factor snail controls epithelial-mesenchymal transitions by repressing E-cadherin expression. *Nat. Cell Biol.* **2**, 76-83.

Carl, T. F., Dufton, C., Hanken, J. and Klymkowsky, M. W. (1999). Inhibition of neural crest migration in Xenopus using antisense slug RNA. *Dev. Biol.* **213**, 101-115.

Collazo, A., Bronner-Fraser, M. and Fraser, S. E. (1993). Vital dye labelling of Xenopus laevis trunk neural crest reveals multipotency and novel pathways of migration. *Development* **118**, 363-376.

Davidson, L. A. and Keller, R. E. (1999). Neural tube closure in Xenopus laevis involves medial migration, directed protrusive activity, cell intercalation and convergent extension. *Development* **126**, 4547-4556.

Deshler, J. O., Highett, M. I. and Schnapp, B. J. (1997). Localization of Xenopus Vg1 mRNA by Vera protein and the endoplasmic reticulum. *Science* **276**, 1128-1131.

Deshler, J. O., Highett, M. I., Abramson, T. and Schnapp, B. J. (1998). A highly conserved RNA-binding protein for cytoplasmic mRNA localization in vertebrates. *Curr. Biol.* **8**, 489-496.

Dibner, C., Elias, S. and Frank, D. (2001). XMeis3 protein activity is required for proper hindbrain patterning in Xenopus laevis embryos. *Development* **128**, 3415-3426.

Doyle, G. A., Bourdeau-Heller, J. M., Coulthard, S., Meisner, L. F. and Ross, J. (2000). Amplification in human breast cancer of a gene encoding a c-myc mRNA-binding protein. *Cancer Res.* **60**, 2756-2759.

Elisha, Z., Havin, L., Ringel, I. and Yisraeli, J. K. (1995). Vg1 RNA binding protein mediates the association of Vg1 RNA with microtubules in Xenopus oocytes. *EMBO J.* **14**, 5109-5114.

Elsdale, T. and Jones, K. (1963). The independence and interdependence of cells in the amphibian embryo. *Symp. Soc. Exp. Biol.* **17**, 257-273.

Epstein, M., Pillemer, G., Yelin, R., Yisraeli, J. K. and Fainsod, A. (1997). Patterning of the embryo along the anterior-posterior axis: the role of the caudal genes. *Development* **124**, 3805-3814.

Essex, L. J., Mayor, R. and Sargent, M. G. (1993). Expression of Xenopus snail in mesoderm and prospective neural fold ectoderm. *Dev. Dyn.* **198**, 108-122.

Farina, K. L., Huttelmaier, S., Musunuru, K., Darnell, R. and Singer, R. H. (2003). Two ZBP1 KH domains facilitate beta-actin mRNA localization, granule formation, and cytoskeletal attachment. *J. Cell Biol.* **160**, 77-87.

Fukuzawa, T. and Ide, H. (1988). A ventrally localized inhibitor of melanization in Xenopus laevis skin. *Dev. Biol.* **129**, 25-36.

Gerhart, J. C. (1979). Mechanisms regulating pattern formation in the amphibian egg and early embryo. In *Biological Regulation and Development* (ed. R. F. Goldberger), pp. 133-316. New York: Plenum Press.

Goto, T. and Keller, R. (2002). The planar cell polarity gene strabismus regulates convergence and extension and neural fold closure in Xenopus. *Dev. Biol.* **247**, 165-181.

Goulding, M. D., Chalepakis, G., Deutsch, U., Erselius, J. R. and Gruss, P. (1991). Pax-3, a novel murine DNA binding protein expressed during early neurogenesis. *EMBO J.* **10**, 1135-1147.

Griffin, D., Penberthy, W. T., Lum, H., Stein, R. W. and Tayler, W. L. (2003). Isolation of the B3 transcription factor of the Xenopus TFIIIA gene. *Gene* **313**, 179-188.

Havin, L., Git, A., Elisha, Z., Oberman, F., Yaniv, K., Schwartz, S. P., Standart, N. and Yisraeli, J. K. (1998). RNA-binding protein conserved in both microtubule- and microfilament- based RNA localization. *Genes Dev.* **12**, 1593-1598.

Heasman, J., Kofron, M. and Wylie, C. (2000). Beta-catenin signaling activity dissected in the early Xenopus embryo: a novel antisense approach. *Dev. Biol.* **222**, 124-134.

Helbling, P. M., Tran, C. T. and Brandli, A. W. (1998). Requirement for EphA receptor signaling in the segregation of Xenopus third and fourth arch neural crest cells. *Mech. Dev.* **78**, 63-79.

Hopwood, N. D., Pluck, A. and Gurdon, J. B. (1989). A Xenopus mRNA related to Drosophila twist is expressed in response to induction in the mesoderm and the neural crest. *Cell* **59**, 893-903.

Ioannidis, P., Trangas, T., Dimitriadis, E., Samiotaki, M., Kyriazoglou, I., Tsiapalis, C. M., Kittas, C., Agnantis, N., Nielsen, F. C., Nielsen, J. et al. (2001). C-MYC and IGF-II mRNA-binding protein (CRD-BP/IMP-1) in benign and malignant mesenchymal tumors. *Int. J. Cancer* **94**, 480-484.

Kislauskis, E. H., Zhu, X. and Singer, R. H. (1994). Sequences responsible for intracellular localization of beta-actin messenger RNA also affect cell phenotype. *J. Cell Biol.* **127**, 441-451.

Kislauskis, E. H., Zhu, X. and Singer, R. H. (1997). beta-Actin messenger RNA localization and protein synthesis augment cell motility. *J. Cell Biol.* **136**, 1263-1270.

Krull, C. E., Lansford, R., Gale, N. W., Collazo, A., Marcelle, C., Yancopoulos, G. D., Fraser, S. E. and Bronner-Fraser, M. (1997). Interactions of Eph-related receptors and ligands confer rostrocaudal pattern to trunk neural crest migration. *Curr. Biol.* **7**, 571-580.

Kwon, S., Abramson, T., Munro, T. P., John, C. M., Kohrmann, M. and

Schnapp, B. J. (2002). UUCAC- and vera-dependent localization of VegT RNA in Xenopus oocytes. *Curr. Biol.* **12**, 558-564.

Leeds, P., Kren, B. T., Boylan, J. M., Betz, N. A., Steer, C. J., Gruppuso, P. A. and Ross, J. (1997). Developmental regulation of CRD-BP, an RNA-binding protein that stabilizes c-myc mRNA in vitro. *Oncogene* **14**, 1279-1286.

Lim, T. M., Lunn, E. R., Keynes, R. J. and Stern, C. D. (1987). The differing effects of occipital and trunk somites on neural development in the chick embryo. *Development* **100**, 525-533.

Linker, C., Bronner-Fraser, M. and Mayor, R. (2000). Relationship between gene expression domains of *Xsnail*, Xslug, and *Xtwist* and cell movement in the prospective neural crest of Xenopus. *Dev. Biol.* **224**, 215-225.

Liu, J. P. and Jessell, T. M. (1998). A role for rhoB in the delamination of neural crest cells from the dorsal neural tube. *Development* **125**, 5055-5067.

Locascio, A. and Nieto, M. A. (2001). Cell movements during vertebrate development: integrated tissue behaviour versus individual cell migration. *Curr. Opin. Genet. Dev.* **11**, 464-469.

Lu, M., Nakamura, R. M., Dent, E. D., Zhang, J. Y., Nielsen, F. C., Christiansen, J., Chan, E. K. and Tan, E. M. (2001). Aberrant expression of fetal RNA-binding protein p62 in liver cancer and liver cirrhosis. *Am. J. Pathol.* **159**, 945-953.

Mayor, R., Young, R. and Vargas, A. (1999). Development of neural crest in Xenopus. *Curr. Top. Dev. Biol.* **43**, 85-113.

Mori, H., Sakakibara, S., Imai, T., Nakamura, Y., Iijima, T., Suzuki, A., Yuasa, Y., Takeda, M. and Okano, H. (2001). Expression of mouse igf2 mRNA-binding protein 3 and its implications for the developing central nervous system. *J. Neurosci. Res.* **64**, 132-143.

Mowry, K. L. (1996). Complex formation between stage-specific oocyte factors and a Xenopus mRNA localization element. *Proc. Natl. Acad. Sci. USA* **93**, 14608-14613.

Mueller-Pillasch, F., Pohl, B., Wilda, M., Lacher, U., Beil, M., Wallrapp, C., Hameister, H., Knochel, W., Adler, G. and Gress, T. M. (1999). Expression of the highly conserved RNA binding protein KOC in embryogenesis. *Mech. Dev.* **88**, 95-99.

Nielsen, J., Christiansen, J., Lykke-Andersen, J., Johnsen, A. H., Wewer, U. M. and Nielsen, F. C. (1999). A family of insulin-like growth factor II mRNA-binding proteins represses translation in late development. *Mol. Cell Biol.* **19**, 1262-1270.

Nielsen, F. C., Nielsen, J., Kristensen, M. A., Koch, G. and Christiansen, J. (2002). Cytoplasmic trafficking of IGF-II mRNA-binding protein by conserved KH domains. *J. Cell Sci.* **115**, 2087-2097.

Nieuwkoop, P. D. and Faber, J. (1967). Normal table of Xenopus laevis (Daudin): a systematical and chronological survey of the development from the fertilized egg till the end of metamorphosis. Amsterdam: North-Holland.

Oleynikov, Y. and Singer, R. H. (2003). Real-time visualization of ZBP1 association with beta-actin mRNA during transcription and localization. *Curr. Biol.* **13**, 199-207.

Regnier, C. H., Masson, R., Kedinger, V., Textoris, J., Stoll, I., Chenard, M. P., Dierich, A., Tomasetto, C. and Rio, M. C. (2002). Impaired neural tube closure, axial skeleton malformations, and tracheal ring disruption in TRAF4-deficient mice. *Proc. Natl. Acad. Sci. USA* **99**, 5585-5590.

Ross, A. F., Oleynikov, Y., Kislauskis, E. H., Taneja, K. L. and Singer, R. H. (1997). Characterization of a beta-actin mRNA zipcode-binding protein. *Mol. Cell Biol.* **17**, 2158-2165.

Ross, J., Lemm, I. and Berberet, B. (2001). Overexpression of an mRNA-binding protein in human colorectal cancer. *Oncogene* **20**, 6544-6550.

Santiago, A. and Erickson, C. A. (2002). Ephrin-B ligands play a dual role in the control of neural crest cell migration. *Development* **129**, 3621-3632.

Sargent, M. G. and Bennett, M. F. (1990). Identification in Xenopus of a structural homologue of the Drosophila gene snail. *Development* **109**, 967-973.

Schroeder, T. E. (1970). Neurulation in Xenopus laevis. An analysis and model based upon light and electron microscopy. *J. Embryol. Exp. Morphol.* **23**, 427-462.

Schwartz, S. P., Aisenthal, L., Elisha, Z., Oberman, F. and Yisraeli, J. K. (1992). A 69 kDa RNA binding protein from Xenopus oocytes recognizes a common motif in two vegetally localized maternal mRNAs. *Proc. Natl. Acad. Sci. USA* **89**, 11895-11899.

Shestakova, E. A., Singer, R. H. and Condeelis, J. (2001). The physiological significance of beta –actin mRNA localization in determining cell polarity and directional motility. *Proc. Natl. Acad. Sci. USA* **98**, 7045-7050.

Smith, A., Robinson, V., Patel, K. and Wilkinson, D. G. (1997). The EphA4 and EphB1 receptor tyrosine kinases and ephrin-B2 ligand regulate targeted migration of branchial neural crest cells. *Curr. Biol.* **7**, 561-570.

Wallingford, J. B. and Harland, R. M. (2001). Xenopus Dishevelled signaling regulates both neural and mesodermal convergent extension: parallel forces elongating the body axis. *Development* **128**, 2581-2592.

Wallingford, J. B. and Harland, R. M. (2002). Neural tube closure requires Dishevelled-dependent convergent extension of the midline. *Development* **129**, 5815-5825.

Wallingford, J. B., Rowning, B. A., Vogeli, K. M., Rothbacher, U., Fraser, S. E. and Harland, R. M. (2000). Dishevelled controls cell polarity during Xenopus gastrulation. *Nature* **405**, 81-85.

Wang, H. U. and Anderson, D. J. (1997). Eph family transmembrane ligands can mediate repulsive guidance of trunk neural crest migration and motor axon outgrowth. *Neuron* **18**, 383-396.

Welch, M. D., Mallavarapu, A., Rosenblatt, J. and Mitchison, T. J. (1997). Actin dynamics in vivo. *Curr. Opin. Cell Biol.* **9**, 54-61.

Yaniv, K. and Yisraeli, J. K. (2002). The involvement of a conserved family of RNA binding proteins in embryonic development and carcinogenesis. *Gene* **287**, 49-54.

Zhang, H. L., Eom, T., Oleynikov, Y., Shenoy, S. M., Liebelt, D. A., Dictenberg, J. B., Singer, R. H. and Bassell, G. J. (2001a). Neurotrophin-induced transport of a beta-actin mRNP complex increases beta-actin levels and stimulates growth cone motility. *Neuron* **31**, 261-275.

Zhang, J. Y., Chan, E. K., Peng, X. X., Lu, M., Wang, X., Mueller, F. and Tan, E. M. (2001b). Autoimmune responses to mRNA binding proteins p62 and Koc in diverse malignancies. *Clin. Immunol.* **100**, 149-156.

Zhang, Q., Yaniv, K., Oberman, F., Wolke, U., Git, A., Fromer, M., Taylor, W. L., Meyer, D., Standart, N., Raz, E. et al. (1999). Vg1 RBP intracellular distribution and evolutionarily conserved expression at multiple stages during development. *Mech. Dev.* **88**, 101-106.